Electronic Supplementary Information

Raman spectrum of Co_3O_4 nanocrystals

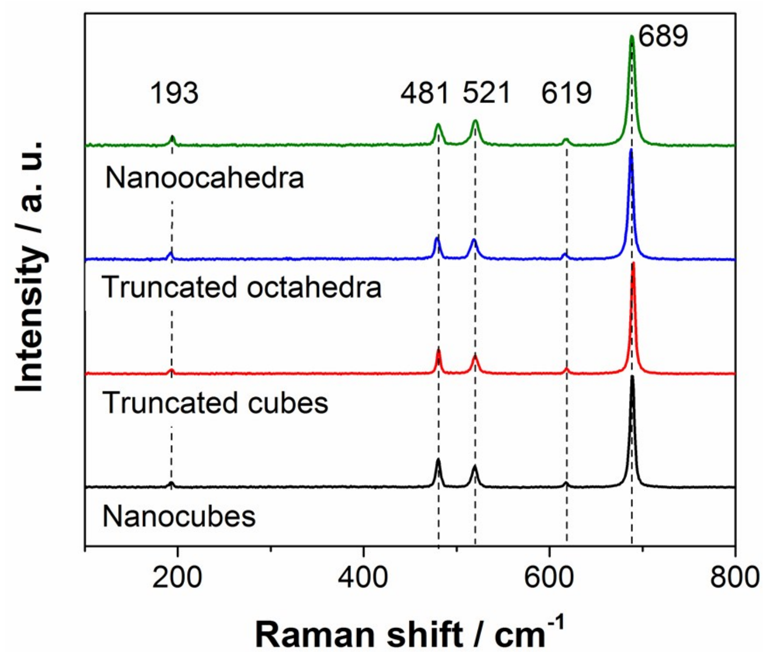

Figure S1. Raman spectra of Co_3O_4 nanocubes, truncated cubes, truncated octahedra and nanooctahedra in powder form. Peaks at 193, 481, 521, 619, and 689 cm^{-1} correspond to the F_{2g}, E_g, F_{2g}, F_{2g}, and A_{1g} vibrational modes, respectively.

Crystal structure of Co_3O_4 and the (100) and (111) surfaces

Co_3O_4 crystal models were constructed using Materials Studio Software. The Crystallographic Information File of Co_3O_4 was obtained from the Inorganic Crystal Structure Database (ICSD #27497). The unit cell structure of Co_3O_4 and the (100) and (111) surfaces are shown in Figure S2. In the two structures on the right, surface cobalt ions are indicated, where the superscripts T and O indicate tetrahedral and octahedral sites, respectively. The subscripts indicate the coordination number. These surface models were constructed according to the work from Zasada et al.[1] The (100) surface has protruding 2-fold coordinated Co^{2+} in tetrahedral sites and 5-fold coordinated Co^{3+} in octahedral sites. The (111) surface is characterized by 3-fold coordinated Co^{3+} ions in octahedral sites and 3-fold coordinated Co^{2+} in tetrahedral sites. The strong under-saturation of the Co^{3+} ions on the (111) surface may be one of the reasons for the higher OER activity of the nanooctahedra.

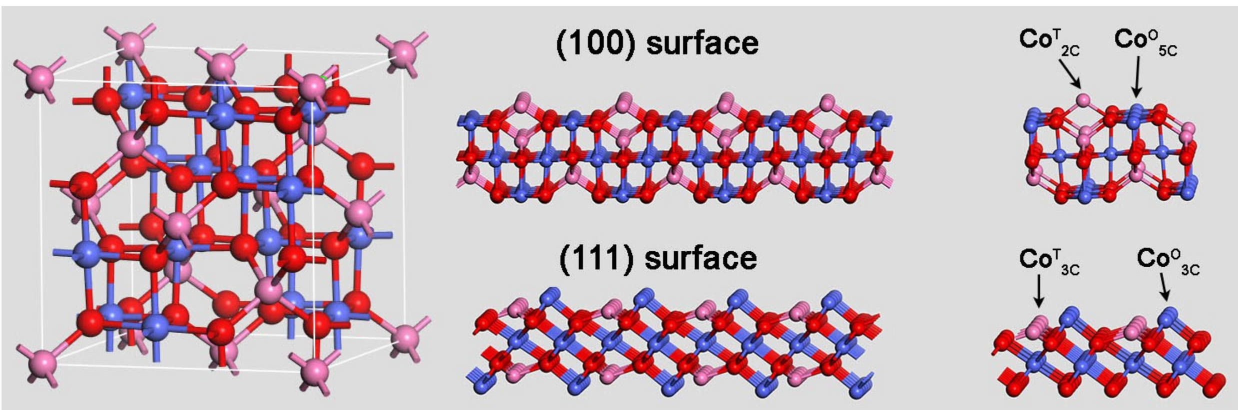

Figure S2. Crystal model of Co_3O_4 and the (100) and (111) surfaces. Rightmost panel shows surface cobalt ions on the (100) and (111) surfaces.

[1] F. Zasada, W. Piskorz, P. Stelmachowski, A. Kotarba, J.-F. Paul, T. Plocinski, K. J. Kurzydlowski, Z. Sojka, J. Phys. Chem. C, 2011, **115**, 6423-6432.

XPS spectra of Co_3O_4 nanocrystals

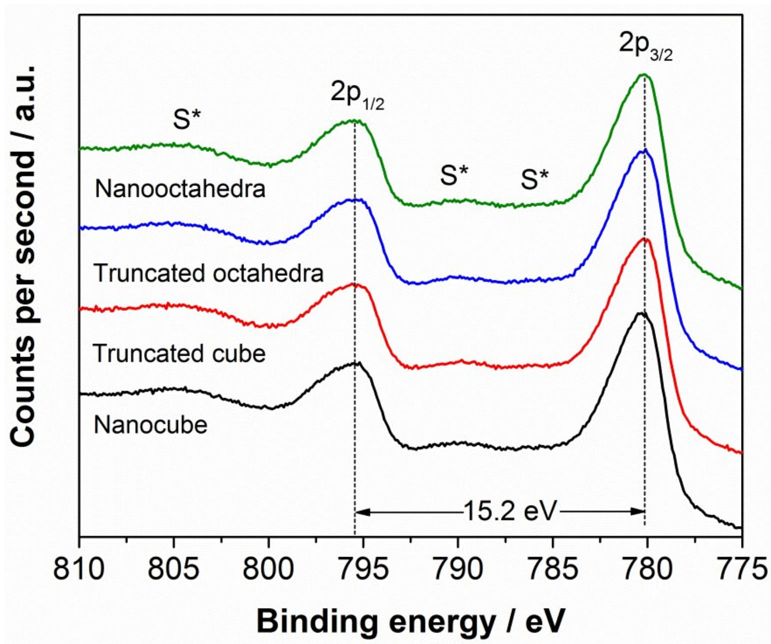

Figure S3. Co 2p XPS spectra of Co_3O_4 nanocubes, truncated cubes, truncated octahedra, and nanooctahedra in powder form.

Faradaic efficiency from RRDE voltammetry

Rotating ring disk electrode (RRDE) voltammetry was performed to confirm the production of oxygen and calculate the Faradaic efficiency. When the working electrode potential is swept anodic, oxygen is generated from the Co_3O_4 surface and is swept towards the platinum ring by the rotating action of the electrode. When the platinum ring is held at -0.5 V vs. Ag/AgCl, it facilitates the reduction of oxygen to hydrogen peroxide through the following reaction:

$$O_2 + 2H_2O + 2e^- \rightarrow H_2O_2 + 2OH^- \qquad \text{(S1)}$$

The Faradaic Efficiency can be calculated from the ring current (I_R), disk current (I_D) and collection efficiency (N) as follows:[2]

$$Faradiac\ Efficiency = \left|\frac{I_R n_D}{N I_D n_R}\right| \qquad \text{(S2)}$$

In Eq. S2, n_D and n_R are the number of electrons transferred in the disk reaction and ring reaction which is 4 and 2, respectively. N is a parameter defined by the geometry of the electrode and has a value of 25.6% according to the manufacturer. Data from RRDE experiments are shown in Figure S4. Based on RRDE experiments, the Faradic efficiency for Co_3O_4 nanocubes and nanooctahedra is 83.3% and 82.1% at 1.7 V vs. RHE. Chou et al reported a Faradaic Efficiency of 95% for 10 nm Co_3O_4 nanoparticles using a fluorescence based oxygen sensor.[3] We believe the discrepancies are due to two factors. First, the particle size and morphologies are very different between our study and the work from Chou et al.[3] Secondly, small oxygen gas bubbles were formed and adhered to the area between the glassy carbon and platinum ring during the RRDE experiments. This could affect the diffusion of oxygen to the platinum ring electrode and result in a smaller ring current and lower Faradaic Efficiency.

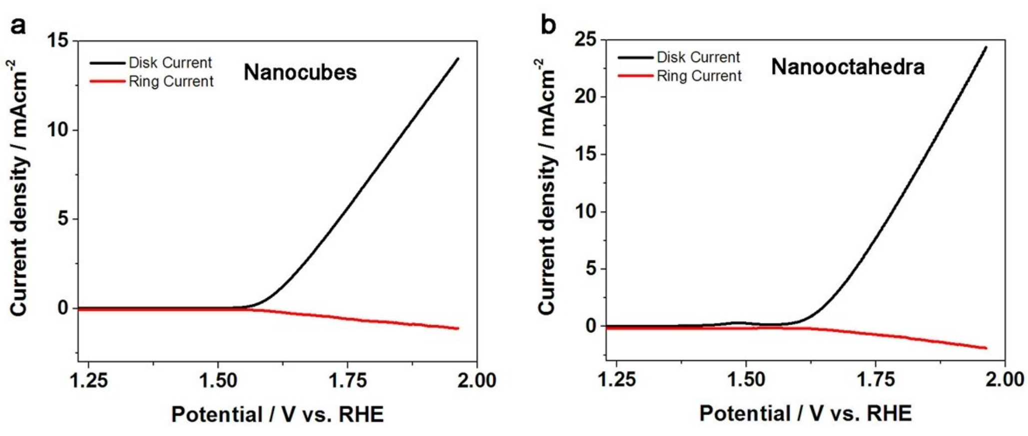

Figure S4 RRDE voltammetry of Co_3O_4 a) nanocubes and b) nanooctahedra.

[2] Y. Liu, S. X. Guo, A. M. Bond, J. Zhang, S. Du, Electrochim. Acta, 2013, **101**, 201-208.
[3] N. H. Chou, P. N. Ross, A. T. Bell, T. D. Tilley, ChemSusChem, 2011, **4**, 1566-1569.

BET surface area analysis

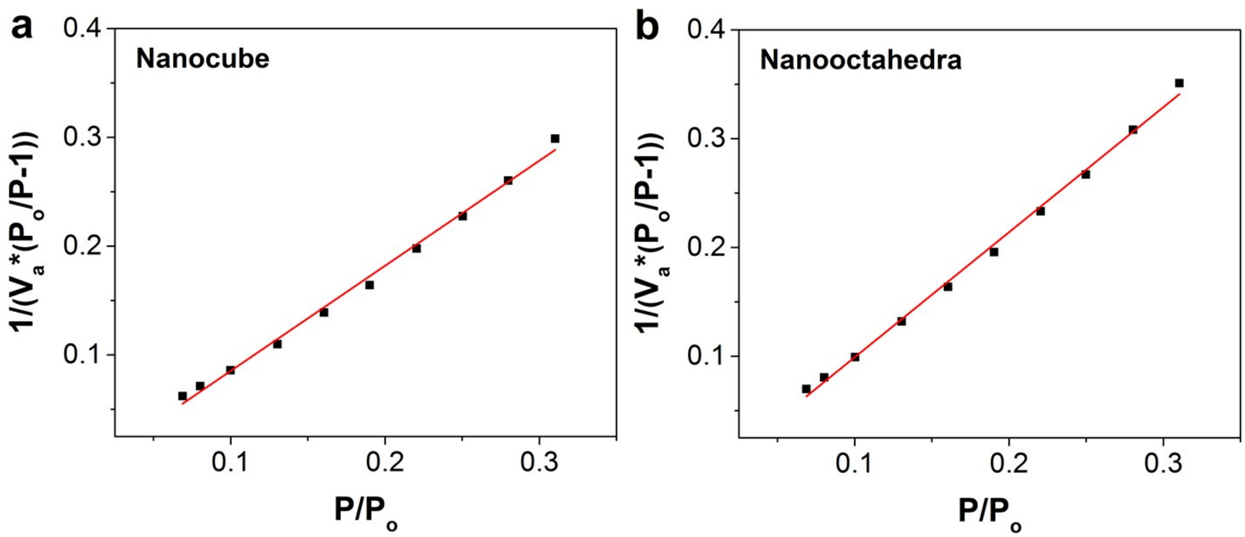

Figure S5. BET multipoint measurements for Co_3O_4 (a) nanocubes and (b) nanooctahedra. The slopes and intercepts from the linear fits (red line) to the data (black dots) were used to calculate the surface area of the nanocrystal samples. Based on these calculations, surface areas for the Co_3O_4 nanocubes was 4.5 m^2g^{-1} and that for Co_3O_4 nanooctahedra was 3.7 m^2g^{-1}.

Capacitance measurement

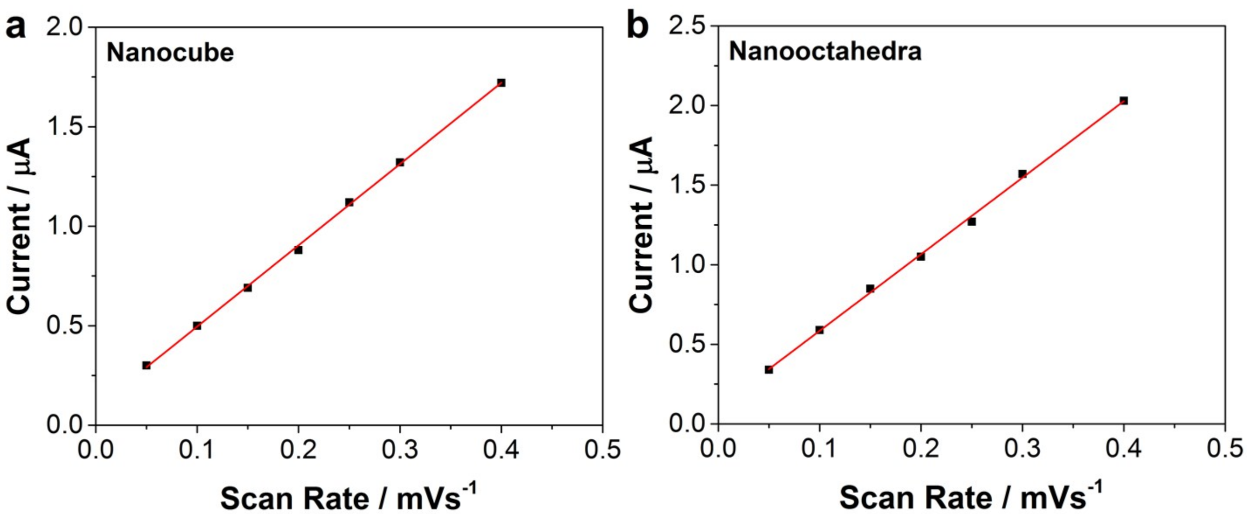

Figure S6. Current as a function of potential-scan rate (a) Co_3O_4 nanocubes and (b) nanooctahedra. The slope of the best fit line (red line) to the data (black dots) can be defined as the capacitance of the catalysts on the glassy carbon working electrode. The capacitance of the Co_3O_4 nanocube modified electrode and nanooctahedra modified electrode was 4.1 and 4.9 μFcm^{-2}, respectively.

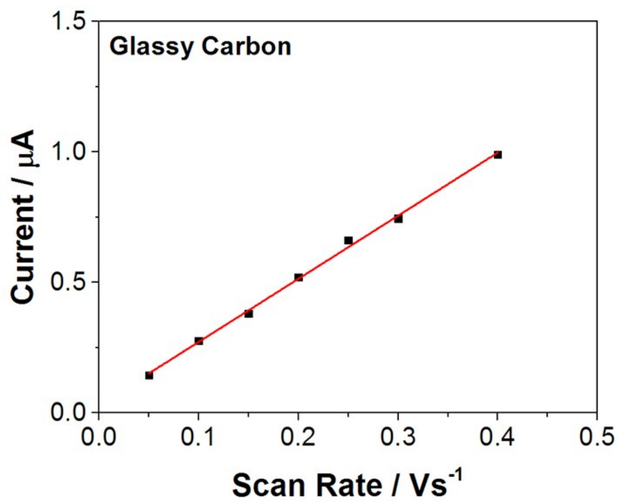

Figure S7. Current as a function of potential-scan rate of clean glassy carbon working electrode. The capacitance of the was 2.4 μFcm^{-2}.

Deconvolution of Co $2p_{3/2}$ XPS spectra

The Co $2p_{3/2}$ XPS spectra of Co_3O_4 nanocrystals in Figure 4 are deconvoluted into five components at 779.8, 781.1, 782.4, 785.1, and 789.1 eV. The first component is due to the main photoelectron lines from Co^{2+} and Co^{3+} ions, and the other component peaks are due to satellite shake-up peaks from either Co^{2+} or Co^{3+} ions. We assigned the components at 779.8 and 782.4 eV to Co^{2+} ions because two peaks at 780.7 and 782.5 eV were observed in the Co $2p_{3/2}$ XPS spectrum of $Co(OH)_2$ obtained by Yang et al.[4] Similarly, we assigned the components at 779.8 and 781.1 eV to Co^{3+} ions because two peaks at 780.4 and 781.7 eV were observed in the Co $2p_{3/2}$ XPS spectrum of CoOOH obtained by Yang et al.[4] Since only Co^{2+} ions are present in $Co(OH)_2$ and only Co^{3+} ions are present in CoOOH, the component at 779.8 eV should be attributed to both Co^{2+} and Co^{3+} while peaks at 781.1 and 782.4 eV are attributed uniquely to Co^{3+} and Co^{2+}, respectively. To deconvolute the Co $2p_{3/2}$ XPS spectra, the peak position and full-width-at-half-maximum (FWHM) were determined by consulting the XPS fitting parameters from the work in Biesinger et al. and Yang et al.[4, 5] The binding energies and FWHM values used for the deconvolution process are tabulated in Table S3.

XPS data obtained at different take-off angles is analyzed by using Eq. S3 that relates the intensity (dI_z) of the detected signal at depth z to the inelastic mean free path (λ) at the signal kinetic energy and the take-off angle (θ) of the detected photoelectron relative to surface normal,[6]

$$dI_z = I_o \exp\left(\frac{-z}{\lambda \cos\theta}\right) dz \tag{S3}$$

where I_o is the intensity of the detected signal that would have been produced if the species probed was at z=0. As a result, it is clear that signal intensity from depth z depends both on θ and the energy. At larger take-off angles, photoelectrons travel through longer distances in the near-surface region which decreases the probed depth and causes higher signal intensity from this region.

[4] J. Yang, H. W. Liu, W. N. Martens and R. L. Frost, J. Phys. Chem. C, 2010, **114**, 111-119.
[5] M. C. Biesinger, B. P. Payne, A. P. Grosvenor, L. W. M. Lau, A. R. Gerson and R. S. Smart, Appl. Surf. Sci., 2011, **257**, 2717-2730.
[6] D. R. Baer, M. H. Engelhard, J. Electron. Spectrosoc. Relat. Phenom., 2010, **178-179**,415-432.

Tables

Table S1. Concentration of reagents used for the synthesis of different Co_3O_4 nanocrystals

	NaOH (M)	$Co(NO_3)_2 \cdot 6H_2O$ (M)
Nanocubes	4.35	1.09
Truncated Nanocubes	2.46	0.82
Truncated Nanooctahedra	2.46	0.41
Nanooctahedra	4.35	0.54

Table S2. Composition of different components of Co $2p_{3/2}$ XPS spectra of Co_3O_4 nanocubes and nanooctahedra.

Nanocubes	Pristine catalyst 0 ° takeoff[a]	Pristine catalyst 60 ° takeoff	After stability test 0 ° takeoff	After stability test 60 ° takeoff
Component 1 779.8 eV	38 %	31 %	42 %	47%
Component 2 781.1 eV	22 %	18 %	21 %	15 %
Component 3 782.4 eV	18 %	27 %	18 %	18 %
Component 4 785.1 eV	16 %	19 %	13 %	14 %
Component 5 789.1 eV	6 %	5 %	6 %	6 %
Nano-octahedra	Pristine catalyst 0 ° takeoff	Pristine catalyst 60 ° takeoff	After stability test 0 ° takeoff	After stability test 60 ° takeoff
Component 1 779.8 eV	40 %	41 %	40 %	41 %
Component 2 781.1 eV	22 %	24 %	20 %	20 %
Component 3 782.4 eV	20 %	13 %	20 %	17 %
Component 4 785.1 eV	13 %	16 %	15 %	16 %
Component 5 789.1 eV	5 %	6 %	5 %	6 %

[a]Zero degree takeoff angle is the emission from the surface normal

Table S3. Fitting parameters for the Co $2p_{3/2}$ XPS spectra of Co_3O_4 nanocubes and nanooctahedra.

Nanocubes	Pristine catalyst 0 ° takeoff[a]		Pristine catalyst 60 ° takeoff		After stability test 0 ° takeoff		After stability test 60 ° takeoff	
	Position (eV)	FWHM (eV)	Position (eV)	FWHM (eV)	Position (eV)	FWHM (eV)	Position (eV)	FWHM (eV)
Component 1 779.8 eV	779.79	1.89	779.75	1.88	779.84	1.92	779.80	1.90

Component 2 781.1 eV	781.13	1.89	780.96	1.88	781.18	1.92	781.11	1.90
Component 3 782.4 eV	782.39	2.54	782.41	2.69	782.33	2.53	782.35	2.34
Component 4 785.1 eV	785.13	4.12	785.40	4.11	785.09	4.12	785.14	4.18
Component 5 789.1 eV	789.10	3.24	789.08	3.37	789.14	3.31	789.20	3.30
Nano-octahedra	Pristine catalyst 0 ° takeoff		Pristine catalyst 60 ° takeoff		After stability test 0 ° takeoff		After stability test 60 ° takeoff	
	Position (eV)	FWHM (eV)	Position (eV)	FWHM (eV)	Position (eV)	FWHM (eV)	Position (eV)	FWHM (eV)
Component 1 779.8 eV	779.83	1.90	779.81	1.89	779.81	1.90	779.82	1.93
Component 2 781.2 eV	781.19	1.90	781.17	1.89	781.19	1.90	781.30	1.93
Component 3 782.5 eV	782.48	2.56	782.51	2.42	782.45	2.61	782.54	2.43
Component 4 785.1 eV	785.13	4.42	784.96	4.51	785.13	4.31	785.21	4.12
Component 5 789.2 eV	789.27	2.98	789.24	3.21	789.31	3.28	789.30	3.29

[a]Zero degree takeoff angle is the emission from the surface normal